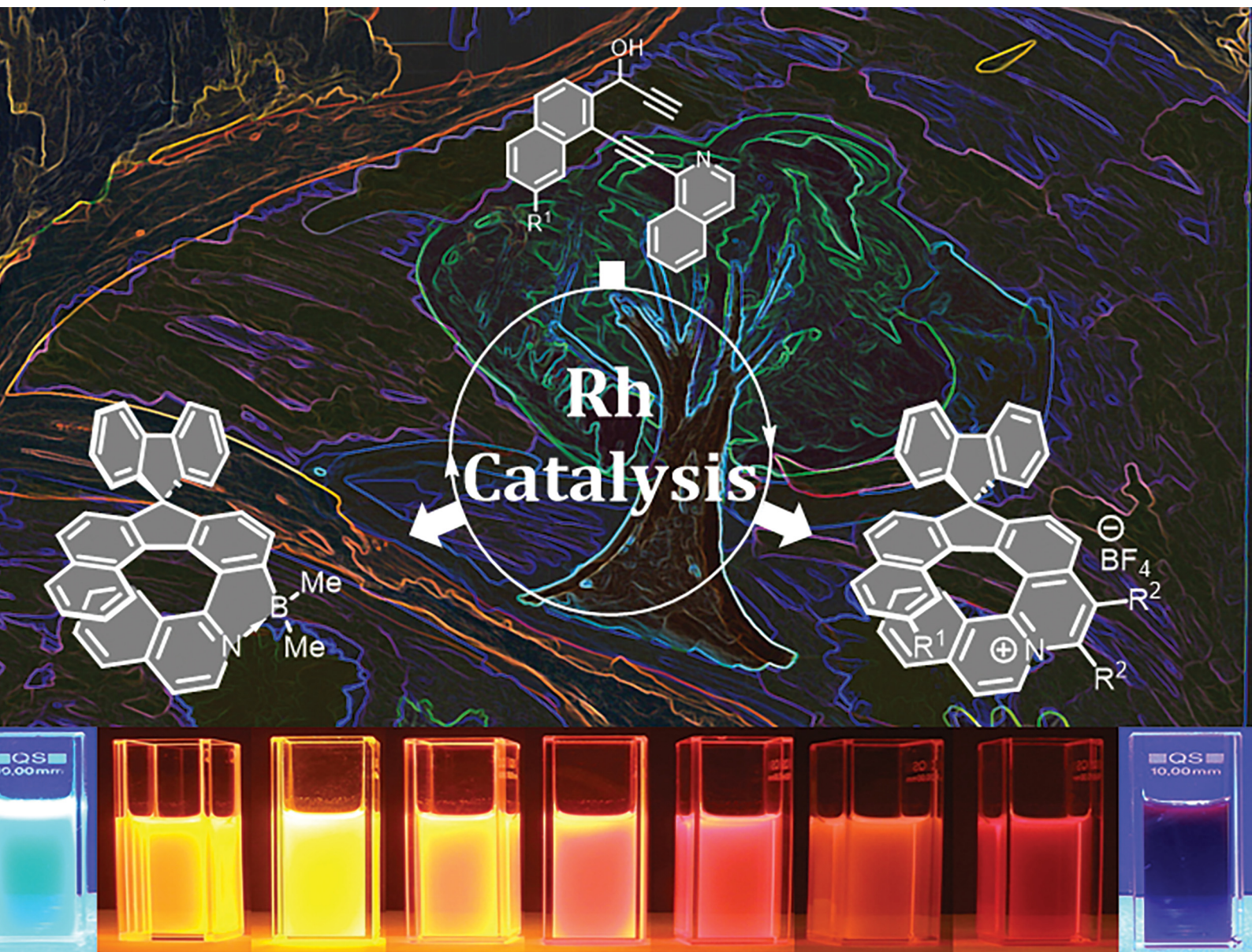


# ChemComm

Chemical Communications

rsc.li/chemcomm



ISSN 1359-7345



Cite this: *Chem. Commun.*, 2025, 61, 4662

Received 11th December 2024,  
Accepted 28th January 2025

DOI: 10.1039/d4cc06512c

[rsc.li/chemcomm](http://rsc.li/chemcomm)

## Synthesis of highly fluorescent helical quinolizinium salts by a Rh-catalyzed cyclotrimerization/C–H activation sequence<sup>†</sup>

Timothée Cadart,<sup>a</sup> Lucia Feriancová,<sup>a</sup> Petr Henke,<sup>b</sup> Robert Gyepes,<sup>c</sup> Ivana Císařová,<sup>b</sup> Květa Kalíková<sup>d</sup> and Martin Kotora<sup>a</sup>  

A series of helical quinolizinium salts were prepared utilizing Rh-catalyzed [2+2+2]cyclotrimerization and C–H activation processes as the crucial synthetic steps. The cyclotrimerization of appropriately substituted diynes with trimethylsilylethyne under Rh-catalyzed conditions provided the 1-arylisquinolines in up to 61% isolated yields. Their Rh-catalyzed C–H activation/annulation with various aryl and alkyl disubstituted alkynes gave rise to [7]-helical quinolizinium salts in high isolated yields (up to 93%). Enantioselective C–H activation was also tried with asymmetric induction up to 62% ee. The respective boron and platinum complexes of 1-arylisquinolines were prepared as well. All prepared compounds exhibit fluorescence in the orange-red light region (606–682 nm) with  $\Phi_f$  28–99%.

Organic helical compounds are a class of substances possessing a curved scaffold composed of alternating *ortho*-fused rings.<sup>1</sup> They have interesting physical properties for potential applications in material science thanks to their twisted shapes and organization in the solid state.<sup>2</sup> Incorporation of heteroatoms into the helicene scaffold has recently emerged as an option to change their structural flexibility and electronic properties, as exemplified by *N*- and *NB*-embedded helicenes.<sup>3–6</sup> One such potential application of helicenes is CPL light emitting materials. However, *[n]*helicenes and their respective heteroatom analogues usually exhibit low fluorescence quantum yields ( $\Phi_f \sim 4\%$ ).<sup>7–10</sup> This can be explained by fast intersystem crossing from the singlet

excited state to the triplet state, which makes them not so attractive for further application in materials science.

In principle, there are three strategies to overcome this problem and increase the quantum yield of compounds with helical scaffolds: (i) introduction of appropriate substituents and/or heteroatoms,<sup>11–13</sup> (ii) lateral extension of the helicene framework,<sup>14–16</sup> and (iii) introduction of a 9,9'-spirobifluorene moiety,<sup>17</sup> because its presence has proved to avoid excimer formation in the solid state.<sup>18</sup> However, it should be kept in mind that the structure–properties relationship between the above-mentioned factors is rather complicated and often combines all the afore-mentioned effects.

We envisioned that the incorporation of an azonia moiety into the helical framework will improve its photophysical properties, because high fluorescence quantum yields ( $\Phi_f$ ) up to 90% were reported for various planar azonia salts.<sup>19–21</sup> Although numerous *[n]*azoniahelicenes (possessing  $\geq 5$  *ortho*-condensed rings) have been synthesized over the last two decades,<sup>22–24</sup> just a handful of data is available regarding photophysical properties.<sup>23,25</sup> As far as introduction of a substituted fluorene moiety in the substrate's molecular framework is concerned, its presence increased  $\Phi_f$  several fold as can be exemplified by a [7]-helical compound ( $\Phi_f = 40\%$ ), with an improvement by almost one order of magnitude.<sup>10</sup> A similar phenomenon was observed for a *B,N*-embedded [6]-helical compound possessing a 9,9'-dimethyl-fluorene moiety ( $\Phi_f = 42\%$ ), where the value for the maternal BN-[6]-helicene was merely 21%.<sup>26</sup> Even higher fluorescence quantum yields (up to 88%) were observed for dispiroindeno[2,1-*c*]fluorenes possessing [5]-, [7]-, and [9]-helical scaffolds.<sup>27–29</sup> Application of the above-mentioned principles may serve design and syntheses of helical compounds having emission maxima in the red or NIR region with reasonably high  $\Phi_{fs}$ , such as an azabuckybowl-helicene hybrid ( $\lambda_{em} = 770$  nm,  $\Phi_f = 28\%$ ),<sup>30</sup> contorted superhelicenes ( $\lambda_{em} = 680$  and 697 nm,  $\Phi_f = 43\%$ ),<sup>31</sup> and naphthalimide-annulated *[n]*helicenes ( $\lambda_{em} = 613$  and 655 nm,  $\Phi_f = 69$  and 73%).<sup>32</sup>

Given our experience with the synthesis of dispiroindeno-fluorenes<sup>27–29</sup> and naphthoquinolizinium salts (Scheme 1a),<sup>21</sup>

<sup>a</sup> Department of Organic Chemistry, Faculty of Science, Charles University, Hlavova 8, 128 00 Praha 2, Czech Republic. E-mail: martin.kotora@natur.cuni.cz

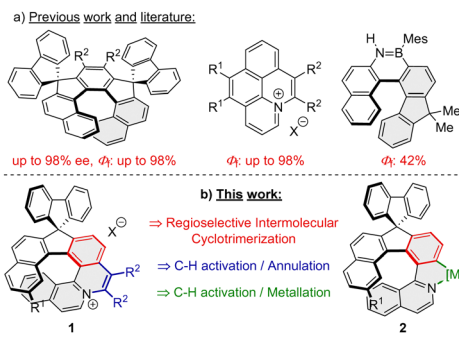
<sup>b</sup> Department of Inorganic Chemistry, Faculty of Science, Charles University, Hlavova 8, 128 00 Praha 2, Czech Republic

<sup>c</sup> Academy of Sciences of the Czech Republic J. Heyrovský Institute of Physical Chemistry, v.v.i. Dolejškova 2155/3, 182 23 Praha 8, Czech Republic

<sup>d</sup> Department of Physical and Macromolecular Chemistry, Faculty of Science, Charles University, Hlavova 8, 128 00 Praha 2, Czech Republic

<sup>†</sup> Electronic supplementary information (ESI) available. CCDC 2373208–2373212. For ESI and crystallographic data in CIF or other electronic format see DOI: <https://doi.org/10.1039/d4cc06512c>

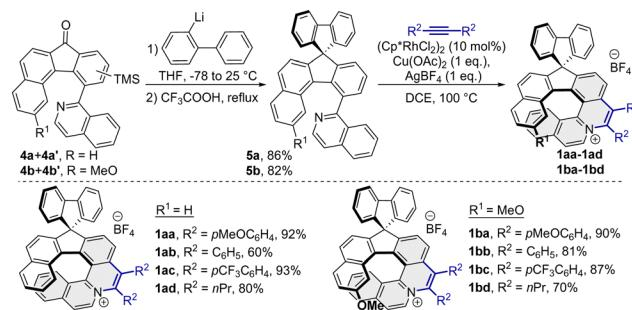




Scheme 1 Previous works (a) and our synthetic proposal (b).

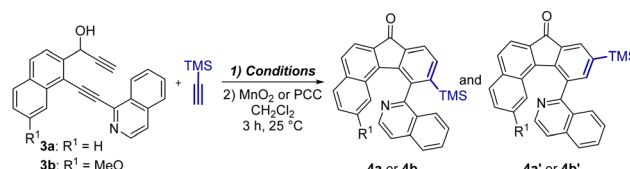
we saw an opportunity in developing a synthetic route towards a new class of compounds that would combine both structural features: the azonia moiety and a helical spirobifluorene fragment. In this report, we would like to demonstrate that the desired helical azonia salts **1** and helical metal complexes **2** (Scheme 1b) can be prepared utilizing two crucial steps relying on transition metal catalyzed reactions: (a) [2+2+2] cyclotrimerization and (b) C-H activation/annulation.

At the outset, we synthesized two diynols **3a** and **3b** bearing the isoquinoline moiety that are the crucial substrates for catalytic [2+2+2] cyclotrimerization from commercially available starting materials in three step synthesis (for details see Section S2, ESI†). Having **3a** and **3b** in hand, screening of different transition metal-based catalysts for the [2+2+2] cyclotrimerization of diynols **3** with trimethylsilylacetylene was carried out (Table 1). The intermediate alcohols were not isolated and directly oxidized to ketones **4** to avoid their rather tedious separation and purification. Using an array of common catalytic systems based on Co, Ni, and Ir complexes to induce cyclotrimerization of **3a** did not provide encouraging results (entries 1–3). Only catalysis by using Rh complexes<sup>33</sup> indicated minor success (entries 4 and 5). According to <sup>1</sup>H NMR analysis of the reaction mixtures, the desired product **4a** was formed in

Scheme 2 Spirocyclization and synthesis of helical quinolizinium salts **1**.

just 5% yield as a mixture of the *ortho* **4a** and *meta* **4a'** regioisomers in 95:5 and 79:21 ratios, respectively. Since we assumed that the low yields could be the result of low solubility of the starting material **3a** in non-polar solvents, the subsequent cyclotrimerizations were carried out in a 1:1 mixture of THF/MeOH. The change of the solvent had a beneficial effect on the course of the reaction and cyclotrimerization of **3a** by using the cationic Rh-complex gave a mixture of **4a** and **4a'** (95:5) in 26% yield (entry 6). Increase of the catalyst loading from 5 to 10 mol% resulted in an improved isolated yield of 59% (entry 7). Gratifyingly, applying the same reaction conditions as in entry 6 provided **4b/4'b** in 61% isolated yield (entry 8). Additionally, isolation and recrystallization of **4a** and **4b** followed by single crystal X-ray diffraction analyses unequivocally confirmed their structures (see Section S5, ESI†).

Since it has been previously shown that a proper choice of ligands around the central metal atom can considerably influence the regioselectivity and yields of catalytic cyclotrimerization,<sup>33–36</sup> the use of different bidentate phosphines was screened (see Section S2.3 and Table S3, ESI†). In general, none of these catalytic systems could match the result obtained with dppb in terms of the yield, albeit the use of BINAP and dppf gave higher preferential selectivity for the formation of **4a** (**4a**:**4a'** = 97:3 in both cases).

Table 1 Screening of various cyclotrimerization conditions of **3** to **4**

Entry <sup>a</sup>	Catalyst (mol%)	Solvent	Temp. (°C)	Yield <sup>b</sup> (%)	<b>4</b> / <b>4'</b>
1	CpCo(P(EtO) <sub>3</sub> )dmfu (10)	Toluene	110	0	
2	Ni(cod)QD (10), PPh <sub>3</sub> (20)	Toluene	110	0	
3	[IrCl(cod)] <sub>2</sub> (10), PPh <sub>3</sub> (20)	Toluene	110	0	
4	Rh(cod) <sub>2</sub> BF <sub>4</sub> (5), dppb (6)	DCE	100	5	95/5
5 <sup>c</sup>	RhCl(PPh <sub>3</sub> ) <sub>3</sub> (10)	THF	170	5	79/21
6	Rh(cod) <sub>2</sub> BF <sub>4</sub> (5), dppb (6)	THF/MeOH	100	26	95/5
7 <sup>d</sup>	Rh(cod) <sub>2</sub> BF <sub>4</sub> (10), dppb (12)	THF/MeOH	100	59 (57) <sup>e</sup>	95/5
8	Rh(cod) <sub>2</sub> BF <sub>4</sub> (5), dppb (6)	THF/MeOH	100	61	98/2

<sup>a</sup> Reaction scale: 0.1 mmol; entries 1–7, **3a:** R<sup>1</sup> = H; entry 8, **3b:** R<sup>1</sup> = OMe. <sup>b</sup> Combined isolated yields. <sup>c</sup> Performed in a MW reactor. <sup>d</sup> 0.25 mmol scale. <sup>e</sup> 1.5 mmol scale.



Next, mixtures of regioisomeric ketones were converted to spirofluorenes **5a** and **5b** in a reaction sequence comprising 1,2-addition of lithiobiphenyl (formed *in situ*) to the carbonyl group followed by intramolecular Friedel–Crafts reaction induced by trifluoroacetic acid under reflux (Scheme 2, the first step). It is worth mentioning that acidic conditions favour not only the intramolecular Friedel–Crafts reaction but also the TMS-desilylation to give only one product **5a** or **5b**. Both spirofluorenes **5a** or **5b** were successfully obtained in high 86% and 82% isolated yields over two steps, respectively.

Then, we proceeded with a rhodium-catalyzed C–H activation/annulation of spirosubstances **5a** and **5b** towards the helical quinolizinium salts (Scheme 2, the second step). Based on our experience, the annulation was performed by using the dimeric rhodium catalyst  $[\text{CpRhCl}_2]_2$  in the presence of  $\text{Cu}(\text{OAc})_2$  and silver salt ( $\text{AgBF}_4$ ) in dichloroethane at 100 °C.<sup>21</sup> Spirocompound **5a** reacted with three symmetric diarylethyynes bearing electron-donating or electron-withdrawing groups ( $p\text{MeO-C}_6\text{H}_4$ , Ph,  $p\text{CF}_3\text{C}_6\text{H}_4$ ), and 4-octyne. The corresponding helical azonia salts **1aa**–**1ad** were formed in high yields (up to 93%). Regarding compound **5b**, the same reaction conditions and reactants furnished products **1ba**–**1bd** in high yields as well (up to 90%).

Then, we attempted conversion of 1-arylisquinoline **5a** to *B,N*- and Pt-embedded helical compounds (Scheme 3), because it has been demonstrated that such substances<sup>37–39</sup> show high appreciation for their potential applications in OLED devices.<sup>40</sup>

As for the former, **5a** was treated with  $\text{BBr}_3$  in the presence of  $i\text{-Pr}_2\text{NEt}$  and the subsequent methylation with trimethylaluminum in toluene provided azabora[7]-helical compound **2a** in a satisfactory yield of 56% (over 2 steps). As for the latter, a two-step reaction sequence starting with **5a** in the presence of  $\text{K}_2\text{PtCl}_4$  in a mixture of ethoxyethanol and water under reflux furnished a platinum dimer, which upon treatment with acetylacetone in the presence of sodium carbonate yielded the expected platinum complex **2b**. Unfortunately, despite all our efforts, the platinum complex **2b** was isolated in only 8% yield so far.

UV/Vis absorption and fluorescence spectra of our [7]-helical quinolizinium salts **1** and complexes **2** in dichloromethane are shown in Fig. 1, the spectral data are summarized in Table 2 (for all details, see Section S4, ESI†). Only small differences in emission maxima in the series of **1aa**–**1ad** and **1ba**–**1bd** were recorded. The emission maxima for the methoxy substituted series **1ba**–**1bd** are bathochromically shifted by 40–50 nm with respect to the unsubstituted series of **1aa**–**1ad**. As far as the substituent effect is concerned, the presence of methoxyphenyl substituents slightly shifts the emissions towards the blue light region (610 nm for **1aa** and 647 nm for **1ba**) with respect to the phenyl substituted derivatives **1ab** and **1bb** (611 and 653 nm,

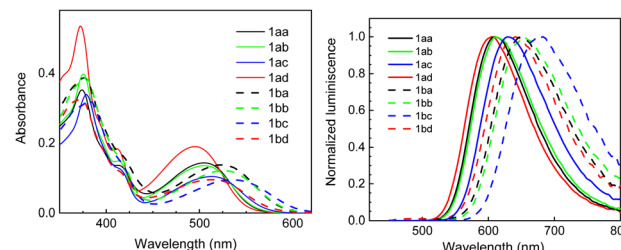


Fig. 1 Normalized absorption and emission spectra of **1** recorded in  $\text{CH}_2\text{Cl}_2$ .

Table 2 Selected photochemical data for **1** in solution ( $\text{CH}_2\text{Cl}_2$ ) and the solid state

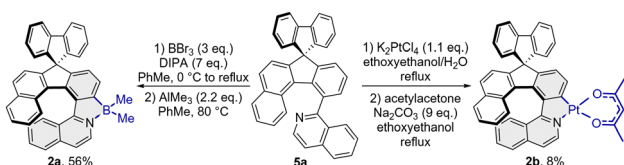
<b>1</b>	$\lambda_{\text{Amax}}$ (nm)	$\epsilon^a$	$\lambda_{\text{Fmax}}^b$ (nm)	$\Phi_f^c$ (%)
<b>1aa</b>	374, 506	18, 7	610 (608)	>99 (62)
<b>1ab</b>	376, 506	19, 6	611 (622)	95 (34)
<b>1ac</b>	379, 514	19, 6	630 (610)	86 (66)
<b>1ad</b>	372, 496	23, 8	606 (614)	91 (21)
<b>1ba</b>	376, 523	21, 7	647 (657)	55 (34)
<b>1bb</b>	378, 525	19, 6	653 (636)	47 (21)
<b>1bc</b>	382, 537	18, 6	682 (676)	28 (24)
<b>1bd</b>	372, 514	15, 4	641 (670)	48 (4)

<sup>a</sup>  $10^3 \text{ M}^{-1} \text{ cm}^{-1}$ . <sup>b</sup> In parentheses are reported  $\lambda_{\text{Fmax}}$  (nm) in the solid state. <sup>c</sup> In parentheses are reported  $\Phi_f$  (%) in the solid state.

respectively), on the other hand the presence of (trifluoromethyl)phenyl substituents shifts the emission maxima towards the red-light region (630 nm for **1ac** and 682 nm for **1bc**). It is worth mentioning that the trend, albeit small, is opposite to the one observed for cationic 11-azapyrrenes,<sup>21</sup> cationic 12-azapryrene,<sup>19,41</sup> and substituted quinolizinium compounds.<sup>42</sup> Concerning the quantum yields, higher  $\Phi_f$  in the range of 86–99% were recorded for **1aa**–**1ad**, whereas for the series possessing the methoxy substituent **1ba**–**1bd** they dropped to 28–55%. All of the compounds also possess a large Stokes shift with values up to 0.491 eV. HOMO → LUMO transitions for **1ba**, **1bb**, and **1bc** were calculated (see the ESI†).

Concerning the metal complexes, azabora compound **2a** shows intense blue-green fluorescence with an emission maximum at 497 nm in  $\text{CH}_2\text{Cl}_2$  and 505 nm in the solid state with quantum yields ( $\Phi_f$ ) up to 34% (see Section 4, Fig. S3 and Table S6, ESI†). Emission maxima for structurally similar azabora-helical compounds were reported to be in the range of 459–477 nm.<sup>37c</sup> On the other hand, the emission maximum of **2b** is significantly shifted by almost 200 nm to the red-light region (690 nm in  $\text{CH}_2\text{Cl}_2$  and 676 nm in the solid state) similarly to the [7]-helical quinolizinium salts **1** (Table 1), but with rather low quantum yield typical for the previously reported Pt(II)-helicene complexes (1–10%).<sup>39</sup>

Compounds **5a** constitutes also a suitable substrate to attempt an enantioselective C–H activation/annulation reaction sequence towards helical azonia salts, which have been shown to proceed with high asymmetric induction as reported by You *et al.*<sup>24</sup> Preliminary experiments of reactions of **5a** and 1,2-bis(4-(trifluoromethyl)phenyl)acetylene as model substrates showed



Scheme 3 Synthesis of helical azabora- and platinum compounds **2**.



that enantioenriched **1ac** could be obtained in 62% ee by using a catalytic system composed of **C1** (10 mol%), AgBF<sub>4</sub> (1 eq.), and Cu(OAc)<sub>2</sub> (1 eq.), but in a low yield of 10% (Section S2.4, ESI†). The level of asymmetric induction is close to the value obtained in the synthesis of a [7]-azomiahelicene, where it reached 73% ee.<sup>24</sup> For full account of preliminary experiments see the ESI,† Section 2.4.

In conclusion, a short synthesis of [7]-helical quinolizinium salts possessing a spirofluorene motif was developed by using a Rh-catalyzed cyclotrimerization and a late stage C–H activation/annulation reaction. In this respect, an appropriately substituted 1-arylisouquinoline motif was a suitable choice for post functionalization and gave us access to a library of helical quinolizinium salts, a platinum complex, and an azabora-compound. Photo-physical properties of the prepared compounds were studied, and these showed high fluorescence ( $\Phi_f$  up to 99% in solution and up to 66% in solid state) with an emission maximum range of 610–690 nm (orange-red light), bathochromically shifted in comparison with the maternal spirofluorenes and indenofluorenes. Furthermore, preliminary attempts on enantioselective annulation were successful with enantioselectivity up to 62% ee. Although these results indicate that reasonable asymmetric induction could be achieved, it is obvious that further extensive fine tuning of the catalyst design will be needed to improve the results.

The authors acknowledge the financial support from the Czech Science Foundation (21-29124S and 21-39639L), the Charles University Research Centre program No. UNCE/SCI/014, and European Structural and Investment Funds (No. CZ.02.2.69/0.0/0.0/18\_053/0016976). We thank Dr Jan Ulč for his help in the synthesis of chiral Cp-complexes.

## Data availability

The data supporting this article are included in the ESI.†

## Conflicts of interest

There are no conflicts to declare.

## Notes and references

- 1 M. Gingras, G. Félix and R. Peresutti, *Chem. Soc. Rev.*, 2013, **42**, 1007–1050.
- 2 M. Gingras, *Chem. Soc. Rev.*, 2013, **42**, 1051–1095.
- 3 For a review on heterohelicenes, see: K. Dhaibi, L. Favereau and J. Crassous, *Chem. Rev.*, 2019, **119**, 8846–8953.
- 4 W.-W. Yang and J.-J. Shen, *Chem. – Eur. J.*, 2022, **28**, e202202069.
- 5 A. V. Gulevskaya and D. I. Tonkoglazova, *Adv. Synth. Catal.*, 2022, **364**, 2502–2539.
- 6 A. Nowak-Król, P. T. Geppert and K. R. Naveen, *Chem. Sci.*, 2024, **15**, 7408–7440.
- 7 A.-C. Bédard, A. Vlassova, A. C. Hernández-Pérez, A. Besette, G. S. Hanan and M. A. Heuft, *Chem. – Eur. J.*, 2013, **19**, 16295–16302.
- 8 H. Kubo, T. Hirose and K. Matsuda, *Org. Lett.*, 2017, **19**, 1776–1779.
- 9 J. Malinčík, S. Gaikwad, J. P. Mora-Fuentes, M.-A. Boillat, A. Prescimone, D. Häussinger, A. G. Campaña and T. Šolomek, *Angew. Chem., Int. Ed.*, 2022, **61**, e202208591.
- 10 H. Oyama, M. Akiyama, K. Nakanmo, M. Naito, K. Nobusawa and K. Nozaki, *Org. Lett.*, 2016, **19**, 3654–3657.
- 11 M. K. Kubitz, W. Haselbach, D. Sretenović, M. Bracker, M. Kleinschmidt, R. Kühnemuth, C. A. M. Seidel, C. Gilch and C. Czekelius, *ChemPhotoChem*, 2023, **7**, e20220334.
- 12 X. Lv, C. Gao, T. Han, H. Shi and W. Guo, *Chem. Commun.*, 2020, **56**, 715–718.
- 13 T. Sakurai, M. Kobayashi, H. Yoshida and M. Shimizu, *Crystals*, 2021, **11**, 1105.
- 14 Z. Qiu, C.-W. Ju, L. Frédéric, Y. Hu, D. Schollmeyer, G. Pieters, K. Müllen and A. Narita, *J. Am. Chem. Soc.*, 2021, **143**, 4661–4667.
- 15 P. Izquierdo-García, J. M. Fernandez-García, S. Medina Rivero, M. Sámal, J. Rybáček, L. Bednárová, S. Ramirez-Barroso, F. J. Ramirez, R. Rodriguez, J. Perles, D. Garcia-Fresnadillo, J. Crassous, J. Casado, I. G. Stará and N. Martin, *J. Am. Chem. Soc.*, 2023, **145**, 11599–11610.
- 16 F. Full, Q. Wölflick, K. Radacki, H. Braunschweig and A. Nowak-Król, *Chem. Eur. J.*, 2022, **28**, e20220228.
- 17 T. P. I. Saragi, T. Spehr, A. Siebert, T. Fuhrmann-Lieker and J. Salbeck, *Chem. Rev.*, 2007, **107**, 1011–1065.
- 18 C. Poriel, C. Quinton, F. Lucas, J. Rault-Berthelot, Z.-Q. Jiang and O. Jeannin, *Adv. Funct. Mater.*, 2021, **31**, 2104980.
- 19 B. Feng, D. Wan, L. Yan, V. D. Kadam, J. You and G. Gao, *RSC Adv.*, 2016, **6**, 66407–66411.
- 20 For a review, see: P. Karak, S. S. Rana and J. Choudhury, *Chem. Commun.*, 2022, **58**, 133–154.
- 21 J. Ulč, J. Jacko, I. Císařová, L. Pospíšil, D. Nečas and M. Kotora, *Eur. J. Org. Chem.*, 2023, e2023001.
- 22 K. Xu, Y. Fu, Y. Zhou, F. Hennersdorf, P. Machata, I. Vincon, J. J. Weigand, A. A. Popov, R. Berger and X. Feng, *Angew. Chem., Int. Ed.*, 2017, **56**, 15876–15881.
- 23 Z. Wang, L. Jiang, J. Ji, F. Zhou, J. Lan and J. You, *Angew. Chem., Int. Ed.*, 2020, **59**, 23532–23536.
- 24 Q. Wang, W.-W. Zhang, C. Zheng, Q. Gu and S.-L. You, *J. Am. Chem. Soc.*, 2021, **143**, 114–120.
- 25 R. Passeri, G. G. Aloisi, F. Elisei, L. Latterini, T. Caronna, F. Fontana and I. S. Sora, *Photochem. Photobiol. Sci.*, 2009, **8**, 1574–1582.
- 26 K. Yuan, D. Volland, S. Kirschner, M. Uzelac, G. S. Nichol, A. Nowak-Król and M. J. Ingleson, *Chem. Sci.*, 2022, **13**, 1136–1145.
- 27 R. P. Kaiser, D. Nečas, T. Cadart, R. Gyepes, I. Císařová, J. Mosinger, L. Pospíšil and M. Kotora, *Angew. Chem., Int. Ed.*, 2019, **58**, 17169–17174.
- 28 T. Cadart, D. Nečas, R. P. Kaiser, L. Favereau, I. Císařová, R. Gyepes, J. Hodáčová, K. Kalíková, L. Bednárová, J. Crassous and M. Kotora, *Chem. – Eur. J.*, 2021, **27**, 11279–11284.
- 29 T. Cadart, T. Gläsel, I. Císařová, R. Gyepes, M. Hapke, D. Nečas and M. Kotora, *M. Chem. Eur. J.*, 2023, **29**, e202301491.
- 30 Y.-F. Wu, S.-W. Ying, L.-Y. Su, J.-J. Du, L. Zhang, B.-W. Chen, H.-R. Tian, H. Xu, M.-L. Zhang, X. Yan, Q. Zhang, S.-Y. Xie and L.-S. Zheng, *J. Am. Chem. Soc.*, 2022, **144**, 10736–10742.
- 31 S. Míguez-Lago, I. F. A. Mariz, M. A. Medel, J. M. Cuerva, E. Maçôas, C. M. Cruz and A. G. Campaña, *Chem. Sci.*, 2022, **13**, 10267–10272.
- 32 X. Tian, K. Shoyama, B. Mahlmeister, F. Brust, M. Stolte and F. Würther, *J. Am. Chem. Soc.*, 2023, **145**, 9886–9894.
- 33 E. Matoušová, R. Gyepes, I. Císařová and M. Kotora, *Adv. Synth. Catal.*, 2016, **358**, 254–267.
- 34 I. Caivano, R. P. Kaiser, F. Schnurrer, J. Mosinger, I. Císařová, D. Nečas and M. Kotora, *Catalysts*, 2019, **9**, 942–950.
- 35 J. M. Halford, A. M. Z. Slawin and A. J. B. Watson, *ACS Catal.*, 2023, **13**, 3463–3470.
- 36 R. Abe, Y. Nagashima, J. Tanaka and K. Tanaka, *ACS Catal.*, 2023, **13**, 1604–1613.
- 37 (a) C. S. Shen, M. Srebro-Hooper, M. Jean, N. Vanthuyne, L. Toupet, J. A. G. Williams, A. R. Torres, A. J. Riives, G. Muller, J. Autschbach and J. Crassous, *Chem. – Eur. J.*, 2017, **23**, 407–418; (b) Z. Domínguez, R. López-Rodríguez, E. Álvarez, S. Abbate, G. Longhi, U. Pischel and A. Ros, *Chem. – Eur. J.*, 2018, **24**, 12660–12668; (c) J. Full, S. P. Panchal, J. Götz, A.-M. Krause and A. Nowak-Król, *Angew. Chem., Int. Ed.*, 2021, **60**, 4350–4357.
- 38 F. Full, M. J. Wildervanck, D. Volland and A. Nowak-Król, *Synlett*, 2023, 477–482.
- 39 E. Anger, M. Rudolph, L. Norel, S. Zrig, C. Shen, N. Vanthuyne, L. Toupet, J. A. G. Williams, C. Roussel, J. Autschbach, J. Crassous and R. Réau, *Chem. – Eur. J.*, 2011, **17**, 14178–14198.
- 40 (a) D. Li, H. Y. Zhang and Y. Wang, *Chem. Soc. Rev.*, 2013, **42**, 8416–8433; (b) Z. Huang, S. Wang, R. D. Dewhurst, N. V. Ignat'ev, M. Finze and H. Braunschweig, *Angew. Chem., Int. Ed.*, 2020, **59**, 8800–8816.
- 41 Q. Ge, Y. Hu, B. Li and B. Wang, *Org. Lett.*, 2016, **18**, 2483–2486.
- 42 W.-M. Yip, Q. Yu, A. Tantipanajaporn, W.-C. Chan, J.-R. Deng and B. C. Ko Wong, *Org. Biomol. Chem.*, 2021, **19**, 8507–8515.

